

## Strengthening of the annual temperature cycle in the mid-latitudes of Northern Hemisphere

Tao Tang<sup>1,2</sup> · Xuhui Lee<sup>3</sup> · Junji Cao<sup>1,2</sup>

Received: 8 September 2024 / Accepted: 25 November 2024

Published online: 09 December 2024

© The Author(s) 2024 [OPEN](#)

### Abstract

The annual temperature cycle (ATC), defined as the surface temperature difference between summer and winter, plays a crucial role in controlling the phenology of biological systems (Sparks and Menzel in *Int J Climatol* 22(14):1715–25, 2002) and in global and regional circulation patterns (Schott and McCreary in *Prog Oceanogr* 51(1):1–123, 2001), (Adam et al. in *J Clim* 29(9): 3219–3230, 2016). Contrary to previous studies which report a decreasing trend in the ATC worldwide (Mann and Park in *Geophys Res Lett* 23(10):1111–4, 1996), (Wallace and Osborn in *Climate Res* 22(1):1–11, 2002), recent studies suggest an increasing ATC trend in the mid-latitude regions (Wang and Dillon in *Nat Clim Chang* 4(11):988–92, 2014). Although the trend may bear anthropogenic fingerprints, the underlying mechanism remains elusive. Using atmospheric reanalysis data and observational records, we confirm that the increasing trend in the ATC occurred during 1980–2020, mainly in the West North America, Mediterranean region and part of North Asia. The main driver of this ATC change is the faster increase in the incoming radiation on the land surface in the summer as a result of the buildup of water vapor and reduction in cloudiness. This increase was further amplified by continental dryness in the summer.

### 1 Introduction

Our understanding of global mean temperature has been extensively documented [7]. However, mean temperature change alone does not provide a complete picture of how the climate responds to anthropogenic influences on the seasonal scale. Seasonality in temperature controls pressure and circulation characteristics, such as the onset of monsoon [2] and the movement of the intertropical convergence zone [3]. It also strongly influences biological events such as flowering date, animal migration and disease infection [1, 8, 9]. These climatic, ecological and health considerations call for detailed characterization of changes in seasonality and drivers of these changes.

One key attribute of seasonality is its magnitude, or the annual temperature cycle (ATC), defined as the surface temperature difference between the summer and the winter. Most previous studies based on observational-records reported a worldwide reduction of the ATC [4, 5, 10, 11]. In contrast to these earlier assessments, recent analyses of observed surface air temperature and tropospheric temperature show that the ATC has been increasing in the mid-latitudes during the past four decades [6, 12]. At these latitudes, summer is now warming faster than winter. The mechanisms, however,

---

**Supplementary Information** The online version contains supplementary material available at <https://doi.org/10.1007/s44288-024-00098-y>.

✉ Tao Tang, [tangtao@mail.iap.ac.cn](mailto:tangtao@mail.iap.ac.cn) | <sup>1</sup>Science Center for Earth System Numerical Simulation, Institute of Atmospheric Physics, Chinese Academy of Sciences, Beijing 100029, China. <sup>2</sup>Key Laboratory of Earth System Numerical Modeling and Application, Institute of Atmospheric Physics, Chinese Academy of Sciences, Beijing 100029, China. <sup>3</sup>School of the Environment, Yale University, New Haven, CT 06511, USA.



remain unclear. In this report, we address this debate by applying a surface energy budget analysis to the ERA5 reanalysis product. We find that faster buildup of water vapor and greater reduction in cloudiness in the summer months than in the winter, respectively, are responsible for the strengthening of the ATC during 1980–2020.

## 1.1 Historical changes in the annual temperature cycle

In our analysis, the ATC is the land surface temperature difference between summer months [June, July and August (JJA) in the Northern Hemisphere (NH) and December, January and February (DJF) in the Southern Hemisphere (SH)] and winter months (DJF in NH and JJA in SH). We define  $\Delta$  as the difference in a quantity between two ten-year periods. For example, the intensification of temperature seasonality in is given as  $\Delta$ ATC, or ATC in 2011–2020 minus ATC in 1980–1989. Four observational temperature datasets, along with ERA5 reanalysis product [13] were employed in the analysis of historical ATC changes (Fig. 1). The observational data include Berkeley temperature data [14], CRUTS-v4 [15], GHCN-version4 [16], and CRUTEM5 [17]. All these data collected temperature records from a large number of ground weather stations and performed homogenization algorithm, as well as rigorous quality control, providing consistent high-quality temperature data over a large fraction of the global land surface. In addition, these datasets are widely used in the climate community, including the latest assessment report of the Inter-governmental Panel on Climate Change [18].

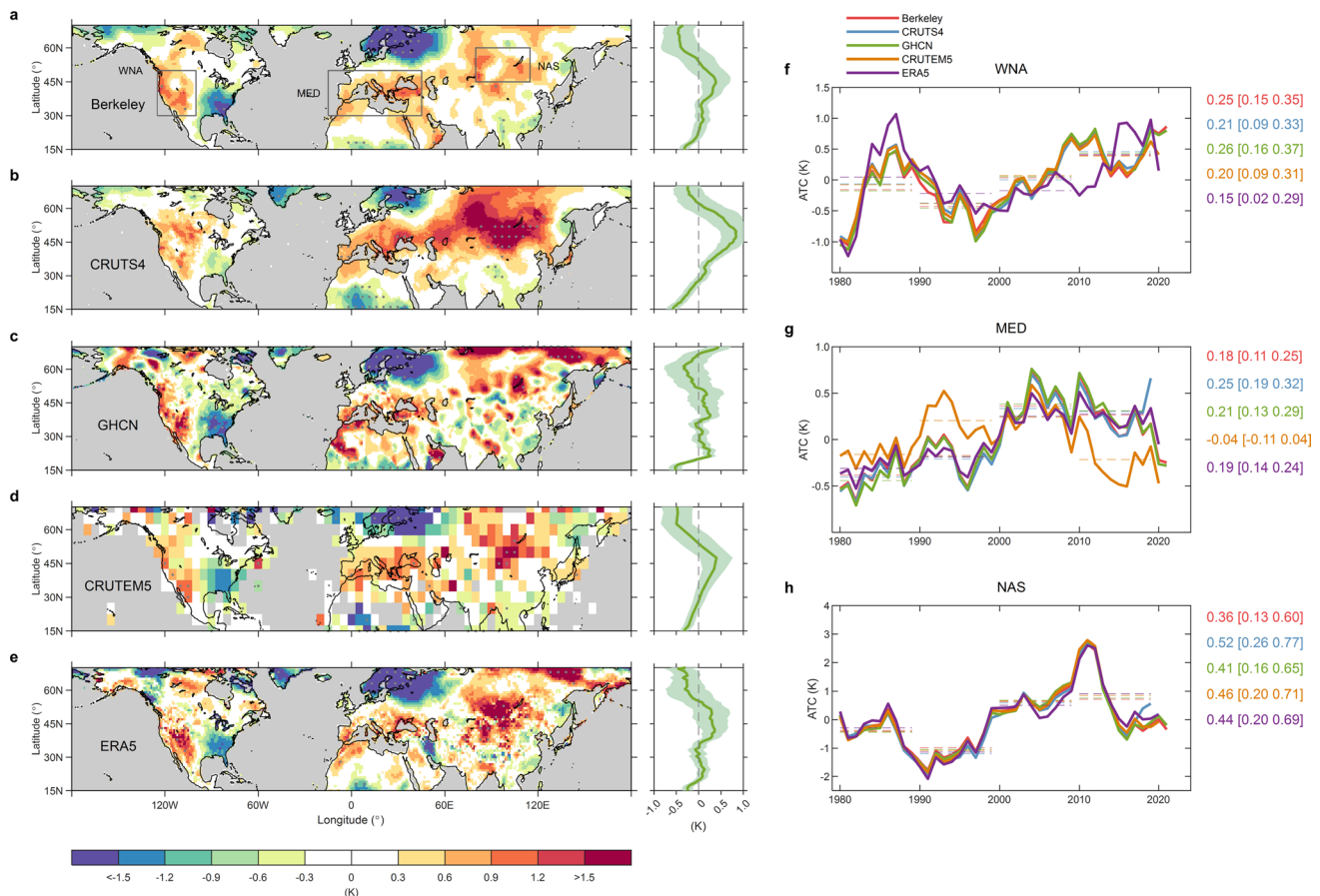


**Fig. 1** Historical change in annual temperature cycle ( $\Delta$ ATC). Spatial map and zonal mean of  $\Delta$ ATC (2011–2020 minus 1980–1989) for **a** Berkeley, **b** CRUTS4, **c** GHCN, **d** CRUTEM5, and **e** ERA5 reanalysis data. **f–g** Domain-averaged time series for West North America (WNA, **f**), the Mediterranean (MED, **g**) and North Asia (NAS, **h**). Gray dots in **a–e** indicate significance at  $p=0.05$  level based on a two-sided student's  $t$  test, which are shown every 5 columns and rows for clarity. Gray boxes in (**a**) mark the three selected regions. In the zonal mean plot, the green lines are the mean change while the shaded regions indicate standard error. In (**f–h**), the linear trends are shown in the right side of each panel in  $\text{K decade}^{-1}$ , with 95% confidence interval being shown for each data in corresponding color. The dashed horizontal lines are decadal mean values of corresponding data. A 5-year moving average was applied to the time series before the trend estimation

Positive  $\Delta\text{ATC}$  is found over most of the regions between 35 and 55°N in all five datasets with varying magnitudes (Fig. 1), with an exception in East North America showing decreasing ATC in all datasets. The zonally positive  $\Delta\text{ATC}$  is mainly contributed by three regions (gray boxes in Fig. 1a), including West North America (WNA, 125°W–100°W, 30°N–50°N), Mediterranean (MED, 15°W–45°E, 30°N–50°N), and North Asia (NAS, 80°E–115°E, 45°N–60°N). The  $\Delta\text{ATC}$  in these regions varies from 0.72 K in MED to 0.91 K in WNA and NAS in the ERA5 dataset. Averaged over these regions, the linear trends range from approximately 0.20 K decade<sup>-1</sup> in WNA and MED to over 0.4 K decade<sup>-1</sup> in NAS, depending on datasets. All these trends are positive with statistical significance at 0.05 level (Fig. 1f–h), except for the MED region in the GHCN data. These pieces of evidence indicate that the positive  $\Delta\text{ATC}$  signal is robust and not sensitive to the chosen dataset.

## 1.2 Surface energy budget analysis

As temperature change is mainly driven by surface radiation change, an energy budget analysis is performed to investigate why ATC increases in these regions (supplementary material). The subscript “cycle” here indicates the seasonal amplitude (summer minus winter) of a quantity. The changes in the seasonal cycle of  $\downarrow\text{LWclear-sky}$  (downward longwave radiation under clear-sky conditions), CRE (cloud radiative effects), and LE (latent heat flux) all contributed to the positive  $\Delta\text{ATC}$  in these regions (Fig. 2a). These three terms, in combination, contributed roughly 64% (WNA), 38% (MED) and 67% (NAS) to the  $\Delta\text{ATC}$  for the indicated regions, respectively. The ratio was estimated as the summation of the three terms in absolute values divided by the summation of all energy terms in absolute values.

It is well established that  $\downarrow\text{LWclear-sky}$  should increase in a warmer climate [19], and contributed almost equally by rising atmospheric temperature ( $T_a$ ) and the buildup of water vapor ( $q$ ) over the globe [20]. Globally,  $T_a$  increased by about same amount ( $\sim 0.5$  K) in winter and summer, but water vapor accumulated faster in the summer relative to the winter (Fig. 2b), thereby enhancing the seasonal cycle of  $\downarrow\text{LWclear-sky}$ . The seasonal cycle of  $q$  increased by 0.9 kg m<sup>-2</sup> in MED and 0.6 kg m<sup>-2</sup> in NAS, but decreased by about 0.3 kg m<sup>-2</sup> in WNA. The increased  $\downarrow\text{LWclear-sky}$  in WNA is therefore completely from a warmer atmosphere.

Although  $q$  increased in the summer, the rate of increase was slower than the rate of increase in saturation humidity. The result is a lower relative humidity and reduced cloudiness [21, 22]. The seasonal amplitude of cloud fraction decreased by as much as 2.7% in WNA and 2.3% in NAS (Fig. 2c). The reduced cloudiness in the summer increases the downward solar radiation (manifested by positive  $\Delta\text{CRE}_{\text{cycle}}$  in Fig. 2a), which enhances warming of the surface layer and contributes to a positive  $\Delta\text{ATC}$ .

The positive contribution of incoming radiation is further amplified by reduced LE in the summer, a phenomenon known as continental drying [21], in which enhanced ET in spring and early summer depletes soil moisture that would otherwise be available for summer months [23, 24]. Consequently, the sensible heat flux  $H$  increases but LE decreases in the summer. Moreover, reduced LE further reduces cloudiness and rainfall [24], which exacerbates solar heating and soil drying, forming a positive feedback that amplifies warming. Continental drying can be quantified by the difference between actual evaporation (ET) and potential evaporation PET (ET–PET). A more negative value of ET–PET indicates a drier climate. Specifically,  $(\text{ET}–\text{PET})_{\text{cycle}}$  becomes more negative in 2011–2020 relative to 1980–1989 in all three regions of interest (Fig. 2d). The reductions span from 0.17 mm day<sup>-1</sup> in NAS to over 0.4 mm day<sup>-1</sup> in WNA and MED. Apart from these three terms,  $\Delta\text{netSWclear-sky}_{\text{cycle}}$  also contributed significantly to the positive  $\Delta\text{ATC}$  in MED (Fig. 2a), which is possibly due to the reduction in aerosol emissions in Europe since 1980s [25]. It is reminded that aerosols have a larger impact on incoming solar radiation during summer months when solar insolation is at its maximum than in the winter. In other words, when aerosol emission was reduced, more solar radiation will reach the surface in the summer months than in the winter.

Finally, we examined whether circulations played a role in the increase of  $\Delta\text{ATC}$ . It is clearly seen that the circulation pattern in NAS region becomes more anticyclonic in the summer than winter (Fig. 2e). This pattern is usually featured with descending air, less cloud fraction, and stronger solar heating [26]. One recent study also reported that ocean activities in Pacific and Atlantic Oceans can excite an atmospheric wave train, leading to an anticyclonic pattern over this region [27]. A similar pattern is also observed over Europe. For WNA, it is in a transition position between cyclonic and anticyclonic conditions, in which the circulations may played a limited role.

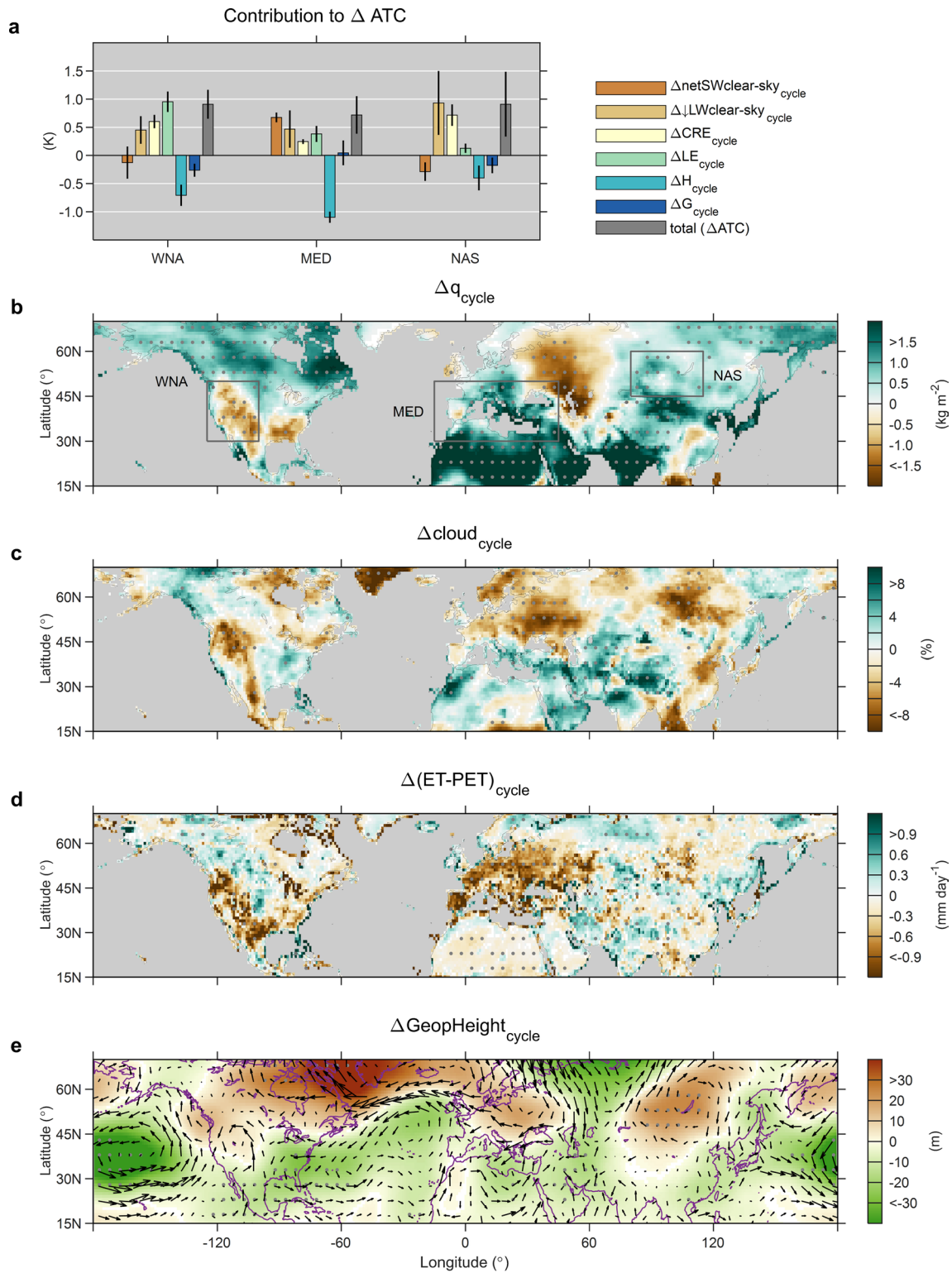


**Fig. 2** Surface energy budget analysis and changes in the seasonal cycle of selected variables between 1980–1989 and 2011–2020 in ERA5 data. **a** Contributions of seasonal cycle of each energy component to  $\Delta$ ATC. Error bars denote one s.e. (**b–e**) Spatial maps for the changes in the seasonal cycle of water vapor ( $\Delta q_{cycle}$ ) (**b**), cloud fraction (**c**), ET deficit (**d**), defined as (ET-PET), and circulations (color shades for geopotential height at 500 hPa and vectors for winds at 850 hPa) (**e**). Gray dots in (**b–d**) indicate significance at  $p=0.05$  level based on a two-sided student's t test, which are shown every 5 rows and columns for clarity

## 2 Discussion

Our analysis shows that changes in the seasonality of downward radiation, mainly  $\downarrow$ LWclear-sky, CRE, and seasonality of latent heat flux contribute to the increasing ATC in the mid-latitudes. The role of the radiation energy stems from a faster buildup of water vapor, more reduction of cloudiness and more dryness in the in the summer months than in the winter. It is noted that our results include the role of circulations and internal variability, as circulations still modify temperature via changing surface radiation. For example, the advection of warm/cold air masses can directly increase/decrease  $\downarrow$ LW radiation. The detailed mechanism of ocean activity or internal variability in modifying the circulations, however, is beyond the scope of the current analysis.

One concern regarding this study is the short analyzing period, in which the multi-decadal internal variability may play a role. We acknowledge that this possibility cannot be ruled out at this stage. In other words, the ATC signal reported above includes both forced response and unforced variability. To what extent, the signal is due to global warming or internal variability merits future investigations. A faster warming summer will be accompanied by more hot extreme events [28], which can have wide-spread serious societal consequences [29–31]. We hope that this report can stimulate more upcoming research on this topic.

**Acknowledgements** We thank the two anonymous reviewers for their constructive and helpful comments in the peer-review process. We acknowledge the support from the Chinese Academy of Sciences (Grant E366363601 and E466301601) and the US National Science Foundation (Grant AGS1933630).

**Author contributions** X.L. and T.T. designed this study. T.T. collected data, performed data analysis and wrote the initial manuscript. All authors contributed to scientific discussion, results framing and manuscript polishing.

**Data availability** All datasets used in this study are freely available from the websites, they include: The ERA5 reanalysis data from European Centre for Medium-Range Weather Forecasts (ECMWF): <https://cds.climate.copernicus.eu/datasets/reanalysis-era5-complete?tab=overview>; Berkeley Earth temperature: <https://berkeleyearth.org/data/>; CRUTS4 temperature analysis and CRUTEM5: <https://crudata.uea.ac.uk/cru/data/temperature/>; GHCN temperature: <https://climatedataguide.ucar.edu/climate-data/ghcn-global-historical-climatology-network-related-gridded-products>. The MATLAB scripts used in the data analysis are available upon reasonable request from the corresponding author.

## Declarations

**Competing interests** The authors declare no competing interests.

**Ethical approval** This article does not contain any studies with human participants performed by any of the authors.

**Open Access** This article is licensed under a Creative Commons Attribution-NonCommercial-NoDerivatives 4.0 International License, which permits any non-commercial use, sharing, distribution and reproduction in any medium or format, as long as you give appropriate credit to the original author(s) and the source, provide a link to the Creative Commons licence, and indicate if you modified the licensed material. You do not have permission under this licence to share adapted material derived from this article or parts of it. The images or other third party material in this article are included in the article's Creative Commons licence, unless indicated otherwise in a credit line to the material. If material is not included in the article's Creative Commons licence and your intended use is not permitted by statutory regulation or exceeds the permitted use, you will need to obtain permission directly from the copyright holder. To view a copy of this licence, visit <http://creativecommons.org/licenses/by-nc-nd/4.0/>.

## References

1. Sparks TH, Menzel A. Observed changes in seasons: an overview. *Int J Climatol*. 2002;22(14):1715–25.
2. Schott FA, McCreary JP. The monsoon circulation of the Indian Ocean. *Prog Oceanogr*. 2001;51(1):1–123.
3. Adam O, Bischoff T, Schneider T. Seasonal and interannual variations of the energy flux equator and ITCZ. Part I: zonally averaged ITCZ position. *J Clim*. 2016;29(9):3219–30.
4. Mann ME, Park J. Greenhouse warming and changes in the seasonal cycle of temperature: model versus observations. *Geophys Res Lett*. 1996;23(10):1111–4.
5. Wallace CJ, Osborn TJ. Recent and future modulation of the annual cycle. *Climate Res*. 2002;22(1):1–11.
6. Wang G, Dillon ME. Recent geographic convergence in diurnal and annual temperature cycling flattens global thermal profiles. *Nat Clim Chang*. 2014;4(11):988–92.
7. Hartmann D et al. Observations: atmosphere and surface, in *Climate change 2013: The Physical Science Basis. Contribution of Working Group I to the Fifth Assessment Report of the Intergovernmental Panel on Climate Change*, T.F. Stoker, et al., Editors. 2013, Cambridge University Press: Cambridge, UK and New York, USA. 159–254.

8. Flockhart DTT, et al. Unravelling the annual cycle in a migratory animal: breeding-season habitat loss drives population declines of monarch butterflies. *J Anim Ecol*. 2015;84(1):155–65.
9. Robert MA, et al. Temperature impacts on dengue emergence in the United States: investigating the role of seasonality and climate change. *Epidemics*. 2019;28: 100344.
10. Qian C, Zhang XB. Human influences on changes in the temperature seasonality in mid- to high-latitude land areas. *J Clim*. 2015;28(15):5908–21.
11. Stine AR, Huybers P, Fung IY. Changes in the phase of the annual cycle of surface temperature. *Nature*. 2009;457(7228):435–40.
12. Santer BD, et al. Human influence on the seasonal cycle of tropospheric temperature. *Science*. 2018;361(6399):eaas8806. <https://doi.org/10.1126/science.aas8806>
13. Hersbach H, et al. The ERA5 global reanalysis. *Q J R Meteorol Soc*. 2020;146(730):1999–2049.
14. Rohde RA, Hausfather Z. The Berkeley earth land/ocean temperature record. *Earth Syst Sci Data*. 2020;12(4):3469–79.
15. Harris I, et al. Version 4 of the CRU TS monthly high-resolution gridded multivariate climate dataset. *Scientific Data*. 2020;7(1):109.
16. Menne MJ, et al. The global historical climatology network monthly temperature dataset, version 4. *J Clim*. 2018;31(24):9835–54.
17. Osborn TJ, et al. Land surface air temperature variations across the globe updated to 2019: the CRUTEM5 data set. *J Geophys Res Atmospheres*. 2021;126(2):e2019JD032352.
18. Trewin B et al. Annex I: Observational Products, in *Climate Change 2021: The Physical Science Basis. Contribution of Working Group I to the Sixth Assessment Report of the Intergovernmental Panel on Climate Change*, V. Masson-Delmotte, et al., Editors. 2021, Cambridge University Press: Cambridge, UK and New York, USA. 2061–2085.
19. Clark JP, et al. Drivers of global clear sky surface downwelling longwave irradiance trends from 1984 to 2017. *Geophys Res Lett*. 2021;48(22):e2021GL093961.
20. Stephens GL, Hu Y. Are climate-related changes to the character of global-mean precipitation predictable? *Environ Res Lett*. 2010;5(2):025209.
21. Wetherald RT, Manabe S. The mechanisms of summer dryness induced by greenhouse warming. *J Clim*. 1995;8(12):3096–108.
22. Boé J, Terray L. Land–sea contrast, soil–atmosphere and cloud–temperature interactions: interplays and roles in future summer European climate change. *Clim Dyn*. 2014;42(3):683–99.
23. Manabe S, Wetherald RT, Stouffer RJ. Summer dryness due to an increase of atmospheric CO<sub>2</sub> concentration. *Clim Change*. 1981;3(4):347–86.
24. Rowell DP, Jones RG. Causes and uncertainty of future summer drying over Europe. *Clim Dyn*. 2006;27(2):281–99.
25. Yang Y, et al. Trends and source apportionment of aerosols in Europe during 1980–2018. *Atmos Chem Phys*. 2020;20(4):2579–90.
26. Meehl GA, Tebaldi C. More intense, more frequent, and longer lasting heat waves in the 21st Century. *Science*. 2004;305(5686):994.
27. Cai Q, et al. Recent pronounced warming on the Mongolian Plateau boosted by internal climate variability. *Nat Geosci*. 2024;17(3):181–8.
28. Rahmstorf S, Coumou D. Increase of extreme events in a warming world. *Proc Natl Acad Sci*. 2011;108(44):17905.
29. De Bono A et al. Impacts of summer 2003 heat wave in Europe. 2004, United Nations Environment Programme. 4 p.
30. Robine J-M, et al. Death toll exceeded 70,000 in Europe during the summer of 2003. *CR Biol*. 2008;331(2):171–8.
31. Gasparrini A, et al. Mortality risk attributable to high and low ambient temperature: a multicountry observational study. *Lancet*. 2015;386(9991):369–75.

**Publisher's Note** Springer Nature remains neutral with regard to jurisdictional claims in published maps and institutional affiliations.